Desalination and Water Treatment
www.deswater.com

doi:10.5004/dwt.2019.23654

145 (2019) 11–25
March

Investigation of phenanthrene degradation in a slurry photocatalytic membrane reactor: Influence of operating variables and data validation

C. Nirmala Rani*, S. Karthikeyan

Centre for Environmental Studies, Anna University, Chennai-600025, India, email: nirmalacrani@gmail.com (C.N. Rani), ksingaram@gmail.com (S. Karthikeyan)

Received 31 May 2018; Accepted 19 December 2018

ABSTRACT

A photocatalytic membrane reactor (PMR) was developed indigenously by integrating a flat sheet ultrafiltration (UF) membrane with a slurry UV-TiO_2 photocatalytic reactor for the removal of phenanthrene (PHE). The effect of operating parameters including initial PHE concentration (1000–1500 µg/L), catalyst dosage (0.1–0.9 g/L) and pH (3.0–9.0) on PHE degradation and TOC removal were investigated. The batch study of the integrated process showed 99.3% PHE degradation and 97.2% TOC removal for optimized values (PHE concentration-1000 µg/L, TiO_2 dosage-0.5 g/L and pH-3) during 3 h reaction while the individual processes; UV-TiO_2 (84% PHE degradation and 60% TOC removal) and membrane separation (53% PHE removal) showed lower removal rates for the same experimental conditions. Lowering the initial PHE concentration was found to increase its percentage removal. The degradation rate of PHE during integrated process (UV-TiO_2 + Membrane) was almost doubled than that during solo photocatalytic process (UV-TiO_2). The PHE degradation followed pseudo-first-order kinetics. The agglomerations of photocatalyst particles were measured by dynamic light scattering (DLS) instrument and the sizes were found to vary between 220–1253 nm for the pH range of 3–9. The obtained experimental results were analysed with response surface methodology (RSM) using Design Expert software. The experimental data showed good agreement with the predicted results obtained from statistical analysis.

Keywords: Phenanthrene; Photocatalysis; Degradation; Mineralization; Kinetics; Modelling

1. Introduction

Polycyclic aromatic hydrocarbons (PAHs) are environmentally persistent organic pollutants (POPs) [1] containing two or more fused benzene rings. They are neutral and non-polar compounds having high melting points, low vapour pressure and low water solubility. With an increase in the number of fused benzene rings, solubility of PAH decreases and hydrophobicity increases. Because of their toxic, mutagenic and carcinogenic effects, 16 PAHs especially those with four or more rings were included in the priority list of pollutants of US EPA and European Union [2,3]. Humans are exposed to PAHs as a part of everyday life because of their ubiquitous nature. The sources of them may be natural or anthropogenic. The natural sources are mainly volcanic eruptions and forest fires [4,5]. Anthropogenic sources are of two types namely pyrogenic (incomplete combustion of fossil fuels, burning of wood, biomass at high temperature) and petrogenic (oil spills from crude and petroleum).

PAHs are one of the main source of pollutant in aqueous matrices including surface, ground and drinking water and wastewaters. Atmospheric deposition, surface runoff, industrial discharges and oil spills causes their presence in surface water. Atmospheric precipitation contributes to 10–80% of the PAHs presence in the oceans [6]. Lipiatou et al. [7] quantified the total PAHs inputs of 47.5 t/year from the atmosphere to the Mediterranean Sea while Rhone and Ebro rivers showed 5.3–33 t/year and 1.3 t/year respectively. The presence of PAHs in ground water may be due to surface water contamination, landfill leachate and agricultural water. Zoller et al. [8] estimated 0.2 and 6.9 ng/L of PAHs in inland waters of the United States and 2.50 ng/L in surface water. The usage of

---

*Corresponding author.

coated pipes of coal tar in water supply systems contribute to the presence of PAHs in drinking water [9]. Several PAHs concentrations were also detected in wastewaters of India [10–12]. Gowri et al. [10] detected the PHE concentration of 1.772 mg/L in Chennai-Nagapattinum coastal water. The water solubility of PHE is 1.6 mg/L. The concentration greater than its water solubility might be due to the presence of organic colloids present in water which would have increased their concentrations beyond their solubility [4,13]. Brindha et al. [11] reported the PHE and acenaphthene (ANA) concentrations of 0.143 and 0.121 mg/L in Chennai-Rayapuram ground water. Malakar and Saha [12] also detected 4.48 mg/L of naphthalene (NAP) in Kolkatta refinery wastewater. Therefore the presence of PAHs are not only the issue of soil and air pollution but also a serious problem of water pollution. Several studies were carried out on photocatalytic degradation of PAHs in aqueous solutions [6,13–15].

Nowadays micropollutants such as PAHs present in the wastewaters are very challenging because of their toxicity even at nanogram level of concentrations. PAHs are non-biodegradable and conventional treatment methods that include coagulation, flocculation, filtration, ozonation and chlorination were found to be ineffective in degrading PAHs in water [6,16]. Though membrane separation and activated carbon reduced the concentrations of these pollutants considerably, several compounds detected in the membrane permeate and effluent of the activated carbon processes indicate the partial removal of these compounds [17]. In addition, the incomplete mineralization during the most effective advanced oxidation processes lead to the presence of the compound intermediates which are more toxic than the parent compound. Considering the toxicity of phenanthrene and its intermediates at lower concentrations in water on humans and animals, it becomes necessary to apply advanced methods that could promote to achieve complete degradation and mineralization of the target compound.

UV photolysis was described to be effective in degrading a wide range of organic micro pollutants. However, direct photolysis using low pressure lamps were limited due to the drawback of the by-products formed whose formation rate and toxicity were higher than the parent compound [16]. Progress in water treatment have led the researchers to the development of photocatalytic processes using semiconductor materials (ZnO, TiO_2 etc.) that can create significant changes in the chemical structure of the pollutants to abate them from aqueous solutions. These processes are called advanced oxidation processes (AOPs) and could be coupled with conventional methods [18]. Due to low cost, small foot print and high efficiency, photocatalysis was recognized as an effective solution to remove PAHs from wastewater [19]. Among the photocatalysts, nanoparticles of TiO_2 were considered to be very effective for the degradation of organic pollutants [20] and several researchers employed nanoTiO_2 as a photocatalyst for the degradation of PAHs [6,13–15]. In this study, we examined the removal of phenanthrene (PHE) which is one of the 16 PAHs classified by USEPA as priority pollutants [21].

During photocatalysis, catalyst applied may either be in the form of powder suspended in slurry or immobilized on various supports such as glass, quartz or stainless steel. The advantages of slurry photoreactor are; high surface area for adsorption and reaction, high degradation rate, no mass transfer limitation and simple reactor configuration. However, the application of slurry reactors are limited due to the additional step of the photocatalyst separation after detoxification. This problem could be overcome by confining or recycling the photocatalyst within the treatment unit [22] by advanced membrane separation in which the membrane acts as a physical barrier against photocatalyst particles and organic molecules or intermediates to be degraded while the separated catalyst can be reused in a slurry photocatalytic reactor and operated continuously [23]. These type of reactors are called photocatalytic membrane reactors (PMRs). PMRs have certain advantages with respect to photoreactors that include: (i) photocatalyst confinement in the reaction environment by means of membrane, (ii) control of residence time of compound molecules in the reactor, (iii) realization of continuous process with simultaneous separation of catalyst and product from the reaction environment, (iv) save energy and reduce the cost of installation for additional operations and (v) possibility of further reuse of catalyst recovered from the reaction mixture.

The PMRs reported in the literatures can be grouped into five categories viz., (i) slurry type of PMR in which photoreactor and membrane unit are placed separately [24]. The membrane employed may be microfiltration (MF) or ultrafiltration (UF) membranes with cross flow filtration, (ii) slurry PMRs in which the photoreactor contains submerged MF/UF membranes with cross flow mode of filtration [25], (iii) slurry PMRs in which the membrane module submerged in the slurry is surrounded by UV lamps placed outside the photoreactor [26], (iv) immobilized PMRs with TiO_2 doped membranes [27] and (v) photocatalytic membrane distillation systems [28]. Though researchers had developed many PMR configurations, slurry reactors confined by means of a submerged flat sheet or hollow fibre membrane seems to be more suitable for practical and industrial applications [26,29,30] and seems to be better solution for the removal of persistent organic pollutants (POPs) such as pharmaceuticals and endocrine disrupting compounds in aqueous solutions [24,26]. In the literature reported PMRs, there are two major drawbacks; (i) non uniform irradiation (light source is placed outside/inside the photoreactor) and (ii) non simultaneous photodegradation and separation (membrane module is kept outside/on one side of the submerged photoreactor) [31]. Moreover, all PMR studies were conducted on either dye or other phenolic compounds. To the best of our knowledge no one study was carried out to evaluate the performance of PMRs on PAHs removal.

Therefore the aim of this study is to evaluate the performance of a novel slurry PMR for PHE removal. This PMR with centrally placed UV-C lamp was designed in such a way to have uniform irradiation. The non-addition of chemicals and the placement of membrane and UV lamp in one unit reduces the installation cost. Since the reject is on the feed side, this particular PMR eliminates the subsequent treatment of wastes that were generated during membrane filtration. Moreover this PMR exhibited good fouling control by means of various adopted fouling control strategies (aeration, periodic cleaning and cross flow filtration).

In this PMR, batch experiments were conducted to assess the effect of initial PHE concentration, TiO_2 dosage and feed solution pH and the process parameters were optimized during individual and combined processes (membrane filtration, UV-TiO_2 and UV-TiO_2 + membrane filtration) for PHE degradation and TOC removals. In addition, this paper also includes a kinetics study of PHE degradation and TOC removals. Response surface methodology with central composite design (CCD) method was employed to assess the interactive effects of various operating variables during integrated process.

2. Materials and methods

2.1. Materials and reagents

Phenanthrene ($C_{14}H_{10}$, MW-178) and titanium oxide (Evonik Degussa P25, Germany TiO_2, 21 nm TEM size) were purchased from Sigma Aldrich. The key physical characteristics of PHE were; molecular weight-178 g/mol; CAS Number-85-01-8 and water solubility-1.6 mg/L. The intrinsic hydrophobicity of these compounds were reflected by their octanol-water partitioning coefficient (Log K_{ow}) values which is 4.46 for PHE. TiO_2 P25 Degussa was a mixture of 70% anatase and 30% rutile with BET surface area 50 m^2/g and band gap 3.2 eV. Hydrochloric acid (36.5–38.0% HCl) and sodium hydroxide (99% NaOH), dichloromethane, acetonitrile and hexane were of HPLC grade purchased from Merck. Double distilled water (Merck) was used for TOC analysis. Reaction mixture was prepared by adding the required concentrations of model compound in distilled water. Required pH was adjusted by 0.1 M NaOH and 0.1 M HCl.

Stock solutions were prepared by dissolving 100 mg of PHE in 100 ml of acetonitrile so that the concentration of the solution was 1000 mg/L. The required concentrations of PHE were obtained from this stock solution. The samples were magnetically stirred to get the homogeneous solution. All glassware used in this experiments were washed with methanol, deionized water and acetone and dried at 110°C for 3 h.

Commercial ultrafiltration (UF) flat sheet membrane of size 305 mm × 305 mm (purchased from Sterlitech Corporation, Kent, WA 98032, USA) was used in fabricating the reactor. This membrane was made up of polyethersulphone (PES) with molecular weight cut-off (MWCO) 100 KDa and the following are the characteristics of the membrane as per the manufacturer: hydrophobic, pH 2–11 and maximum flux 693–741 ml/min for 50 psi.

2.2. Experimental setup

The schematic diagram of the developed laboratory scale slurry PMR is shown in Fig. 1. The reactor of 2.1 L volume consisted of a UV-C lamp (Philips TUV 16 W, λ_{max} = 254 nm, irradiation intensity = 1.54 W/m^2) and a flat sheet polyethersulphone (PES) YMLY3001 - Synder LY Membrane (size 305 mm × 305 mm and MWCO 100 KDa purchased from Sterlitech Corporation, Kent, WA 98032, United States of America). The flat sheet membrane was rolled into a cylinder of 97 mm diameter and 305 mm height and placed between two stainless steel perforated sheets and fixed on a flange plate at the bottom. In this type of set up, the reaction mixture remains inside the membrane and since the reject is on the feed side, there is no separate reject stream. In order to provide uniform irradiation,UV lamp was placed at the centre of the rolled membrane. The lamp which was in direct contact with the aqueous solution was protected by a double layered quartz glass tube through which water was recirculated. In order to collect the membrane permeate, the reactor was surrounded by an outer vessel made up of Plexiglas. An air diffuser plate was provided at the bottom of the reactor for which an air pump was connected.

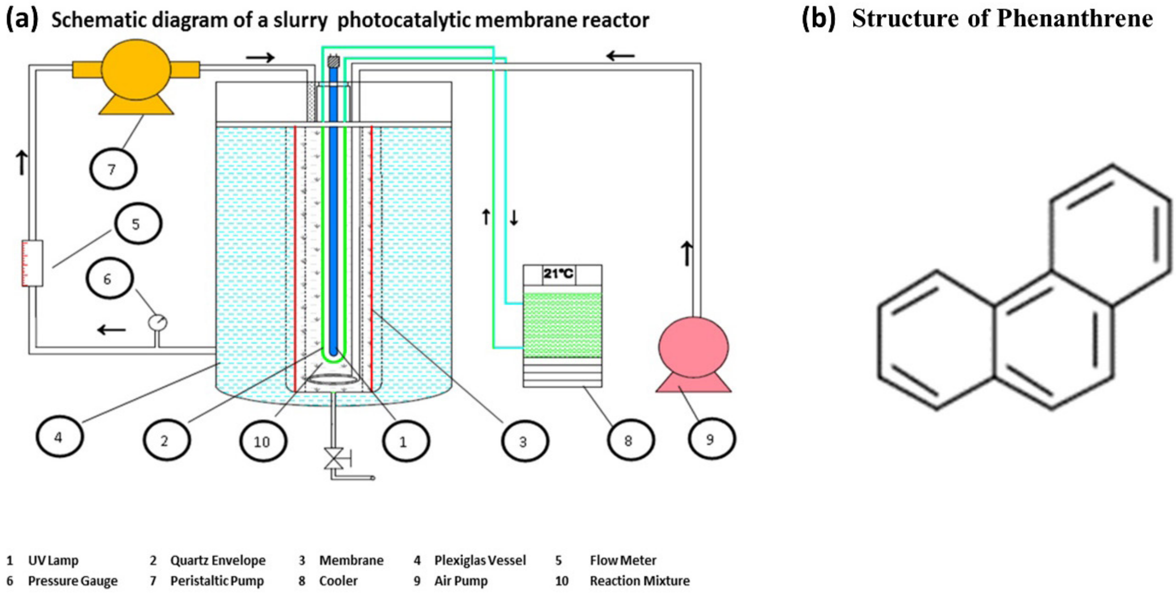

Fig. 1. The experimental setup of the photocatalytic membrane reactor (PMR).

2.3. Analytical methods and measurements

2.3.1. Experimental procedure

The batch studies were carried out in a 2.1 L of reaction mixture containing known concentrations of PHE and TiO_2 in distilled water. Prior to the experiment, the reaction mixture was continuously stirred in dark environment for 30 min in order to reach adsorption equilibrium of PHE on the catalyst's surface. Batch studies were carried out with different initial concentrations (1000–1500 µg/L) of PHE. After optimizing the pollutant concentration (1000 µg/L), pH of the reaction mixture was varied from 3–9 and optimized. Permeates were withdrawn at 31 mL/min (flux 20 $L/m^2 h$) and recycled back into the reactor. To separate the photocatalyst particles from the solution, samples were collected at 30 min interval and centrifuged at a speed of 4000 rpm for 5 min. In order to produce the reproducibility of the results, each experiment was performed at least twice. This PMR system was continuously aerated at a flow rate of 1.5 L pm since higher aeration rates produce greater shear rates and prevent agglomeration of photocatalyst particles which in turn increases the availability of surface area for the degradation of the compounds [32].

2.3.2. Degradation and mineralization study

To minimize photolytic decomposition, samples and the standards were stored in amber bottles. The concentrations of PHE in the samples taken from the reactors were quantified by gas chromatography (GC) mass spectrometry (MS) detection after concentrating the sample by liquid-liquid extraction (LLE). The mineralization efficiency was determined by analysing the TOC of the samples using TOC-VCPH/CPN PC-controlled TOC Analyser (SHIMADZU Corporation, KYOTO, Japan) with an NDIR detector (680ºC combustion catalytic oxidation technique). The repeatability of the measurements from GC-MS and TOC analyser was checked by standard deviation (SD) and coefficient of variation (CV). The errors in measurement for all samples were estimated to be within ± 5%. PHE degradation percentages were calculated using Eq. (1):

$$\text{PHE Degradation (\%)} = \frac{[C_0 - C_t]}{[C]_0} \times 100 \tag{1}$$

where C_0 = initial PHE concentration and C_t =final PHE concentration.

2.3.3. Analysis of TiO_2 particle size

TiO_2 agglomerations in this work were measured using Dynamic Light Scattering (DLS) instrument ZEN 3600, He-Ne laser (633 nm). The size range that could be measured using this instrument is 0.3 nm to 10000 nm.

2.3.4. Experimental design data analysis

To optimize the PHE degradation and TOC removal, response surface methodology (RSM) based upon central composite design (CCD) was employed. The three factors/parameters; Initial PHE concentration, TiO_2 dosage and pH were assessed for two responses; PHE degradation and TOC removal. The obtained experimental data was analysed by Design-Expert software.

3. Results and discussion

3.1. PHE-TiO_2 adsorption in the dark and PHE photolysis

At the first step of experimentation, dark control tests were carried out to evaluate the possible adsorption of PHE on TiO_2 photocatalyst. For dark adsorption, 2.1 L sample containing 1000 µg/L PHE and 0.5 g/L TiO_2 was covered with aluminium foil sheet and kept for 24 h in a dark environment. The initial pH of the sample was the sample pH (6.1) and was not modified. The sample was analysed for PHE concentration and the results showed that only 8% of PHE molecules were adsorbed onto TiO_2 surface which may be due to the effect of electrostatic repulsion. Moreover, the extent of UV-C photolysis on PHE degradation was evaluated by recycling batch experiments for 3 h (in the absence of UF module and TiO_2 nano particles) and was found to be 34%. Similar results were observed by others [16,33]. Sanches et al. [16] investigated the degradation of 3 PAHs namely anthracene (ANT), fluoranthene (FLU) and benzo [a] pyrene [BaP] using low pressure UV lamps of 254 nm and observed the percent degradation of 48%, 13% and 36% on surface waters after 2.5–3.2 h, 2.5–2.9 h and 3.6–4.6 h of irradiation respectively. Zhu et al. [33] carried out UV photolytic experiments on 5 g soil samples using two UV lamps of 254 nm (irradiation time 5 days) for the degradation of PHE and reported the percent degradation of approximately 32%. In order to appropriately design the main experiments and to minimize the errors due to non-photocatalytic phenomena such as adsorption and photolysis, these tests were conducted.

3.2. Membrane separation experiments

Experiments on membrane separation were carried out by varying initial PHE concentrations (1000, 1100, 1300, 1400 and 1500 µg/L) and pH (3, 6.1, 7 and 9). Samples were taken at a time interval of 30 min for 3 h and samples were analysed. The obtained results are depicted in Fig. 1S (supplementary content). In this study, the maximum removal of PHE during membrane separation was found to be 53%. There are two possible explanations for PHE removal.

Size exclusion and adsorption are the two phenomena responsible for the reduction in pollutant concentration during membrane separation [24]. In this study, since the molecular size of PHE is lesser than the pore size of the membrane, size exclusion did not favour for the reduction in PHE concentrations. Therefore, the reduction in PHE concentrations could be due to adsorption of PHE molecules on the membrane surface alone. This is one reason for compound removal. The other reason for PHE removal could be explained with respect to the hydrophobicity of the membrane. Since PHE molecules are hydrophobic and having higher log K_{ow} (4.46) value greater than 4, the membrane might have retained the PHE molecules and favoured the removal [26,34,35]. Similar observations were made by others [36–38]. Luks-Betlej and Dudziak [36] investigated the removal of PAHs (initial concentrations: 55 to 2300 mg/

dm^3) using NF membrane and noticed 90% removals. Smol and Wlodarczyk-Makula [37] investigated the percent degradation of PAHs using UF membrane (pore size 0.04 µm) and reported that nearly 66.6% of PAHs could be removed by the UF membrane when the initial concentrations of PAHs were 8.9–19.3 mg/L. Another study carried out by Gong et al. [38] revealed that UF membrane with 5000 Da MWCO could be able to remove 42.5% of PAHs. All the above studies reported that the removal mechanism during membrane separation was due to adsorption of PAH molecules on the membrane surface.

3.3. UV photocatalytic experiments

Photocatalytic experiments were performed by varying PHE concentrations (1000, 1100, 1300, 1400 and 1500 µg/L), TiO_2 dosage (0.1, 0.3, 0.5, 0.7 and 0.9 g/L) and pH (3, 6.1, 7 and 9). Samples were collected at a time interval of 30 min, centrifuged, decanted and analysed. In this study, the maximum degradation of PHE during UV photocatalytic experiments was found to be 84%. The results obtained in this study could be compared with the results of others [13,15]. Lin and Valsaraj [13] examined the degradation of PAHs in dilute water streams (20 nm Degussa P25 [TiO_2] = 2.128 g, [PHE] = 0.838 g, 4 UV lamps of 8.1 mW/cm^2) and found that only 67% PHE was degraded during 3 h irradiation. Liu et al. [15] investigated the degradation of PAHs in offshore produced water (1.2 L reaction mixture, 3 UV-C lamps 254 nm, 3.7–3.8 mw/cm^2, 13.5 nm nano [TiO_2] = 0.05 g, [16 PAHs] = 500 µg/mL) reported that PAHs with less than 4 aromatic rings had *k* values higher than 0.0005/min indicating that more than 50% of the compound was destructed within 24 h. PAHs were not completely degraded during photocatalytic oxidation (PCO). However, the addition of oxidants H_2O_2 [39] and $Na_2S_2O_8$ [6] and acetone [40] enhanced the degradation rate up to certain extent.

The results obtained from the individual processes (membrane separation and UV-TiO_2) and the above discussed research results reveal that only partial removal of PHE could be possible during individual processes and hence made the necessity to go for integrated processes in order to achieve complete degradation and mineralization of the target compound.

3.4. PHE removal in photocatalytic membrane reactor

3.4.1. Effect of photocatalyst loading

The previous studies reveal that PAHs undergo efficient photodegradation by TiO_2 [14,41,42]. The effect of catalyst loading on photodegradation of PHE was studied by many researchers [6,14]. In this study, the effects of TiO_2 loading on PHE and TOC removals were investigated in a batch reactor for the dosages of 0.1, 0.3, 0.5, 0.7, 0.9 g/L and the results are shown in Fig. 2 (a and b). It is very much interesting to note that for the variations of TiO_2 dosages from 0.1 g/L to 0.5 g/L, the PHE (57–99%) and TOC (52–97%) removals increased and reached the maximum percentages of 99% and 97% respectively. The possible explanation could be; increase in catalyst load increased the surface area on which large number of photons and compound molecules were absorbed. On the other hand, increasing the catalyst loading from 0.5 to 0.9 g/L, decreased the percent removal of PHE to 50%. This may be due to light scattering effect and particle aggregation [43,44]. When suspended in water, due to agglomeration, the size of the catalyst particles increases from nm to µm. The agglomerated sizes were measured by Dynamic Light Scattering (DLS) instrument and the sizes are depicted in Figs. 3 a–c. In this studyTiO_2 particle sizes varied from 220 to 1253 nm. These results were in coincidence with the particle sizes reported by others [26,42,43] in which the TiO_2 agglomerations were measured to be in the range from 200 to 1200 nm. The particle agglomeration and particle to particle interaction would have reduced the available active sites for surface holes and electrons and reduced the degradation and mineralization efficiencies. Furthermore, the increase in catalyst loading increased the turbidity of the reaction mixture and reduced the light intensity in the solution which in turn reduced the concentration of photogenerated holes and electrons. This also could be the reason for the reduction in photocatalytic efficiency of the process. For practical applications, in order to avoid the unnecessary excess of catalyst and to ensure total absorption of efficient photons the optimum dosage of catalyst should be chosen [44]. The maximum percentage of PHE degradation and TOC removals were achieved at 0.5 g/L of TiO_2 and this was found to be the optimum dosage for the experimental condition.

In this study, the recirculating fluid contained more catalyst particles at the beginning and reduced later. The initial feed turbidity (for 0.5 g/L of TiO_2) was 3010 NTU. Though the turbidity of permeate was 30–35 NTU at the beginning, after 3 h, the turbidity of permeate dropped to 0.19–0.22 NTU. The reductions in permeate turbidity may be due the retention of agglomerated catalyst particles (agglomerations were measured by DLS and shown in Fig. 3) on the feed side. The permeate turbidity measurements obtained in this study could be compared with the observations of others. Sopajaree et al. [45] employed a PES UF membrane with 100 KDa MWCO in PMR and noticed a permeate turbidity of 0.22 NTU to 0.42 NTU for which the feed turbidity was 5200 NTU (corresponds to the TiO_2 dose of 1 g/dm^3) after 35 min of operation of PMR. Mozia et al. [46] employed polysulfone UF membrane with MWCO 500 KDa and observed that the initial turbidity of the feed 2100 NTU (corresponds to TiO_2 dose of 0.3 g/L) dropped to 0.08 NTU in permeate after 5 h.

3.4.2. Effect of feed pH

pH is one of the main factors influencing the degradation rate of organic compounds during photocatalytic process [47] and in heterogeneous photocatalytic process, pH affects the surface charge of the photocatalyst, size of the catalyst aggregates as well as the position of the valence and conduction band [24,30,48]. The effect of pH on photodegradation of PHE was studied by varying pH of feed solution (3, 5, 6.1 and 9). The feed pH was adjusted by adding 0.1 M NaOH or 0.1 M HCl during experimentation. The results obtained are demonstrated in Figs. 2c and d and the results reveal that the feed pH had significant effect on PHE degradation. High degradation of 99% was obtained at pH = 3 and at pH = 9, lower percentage removal of 71% was obtained. The effect of feed pH parameter on integrated

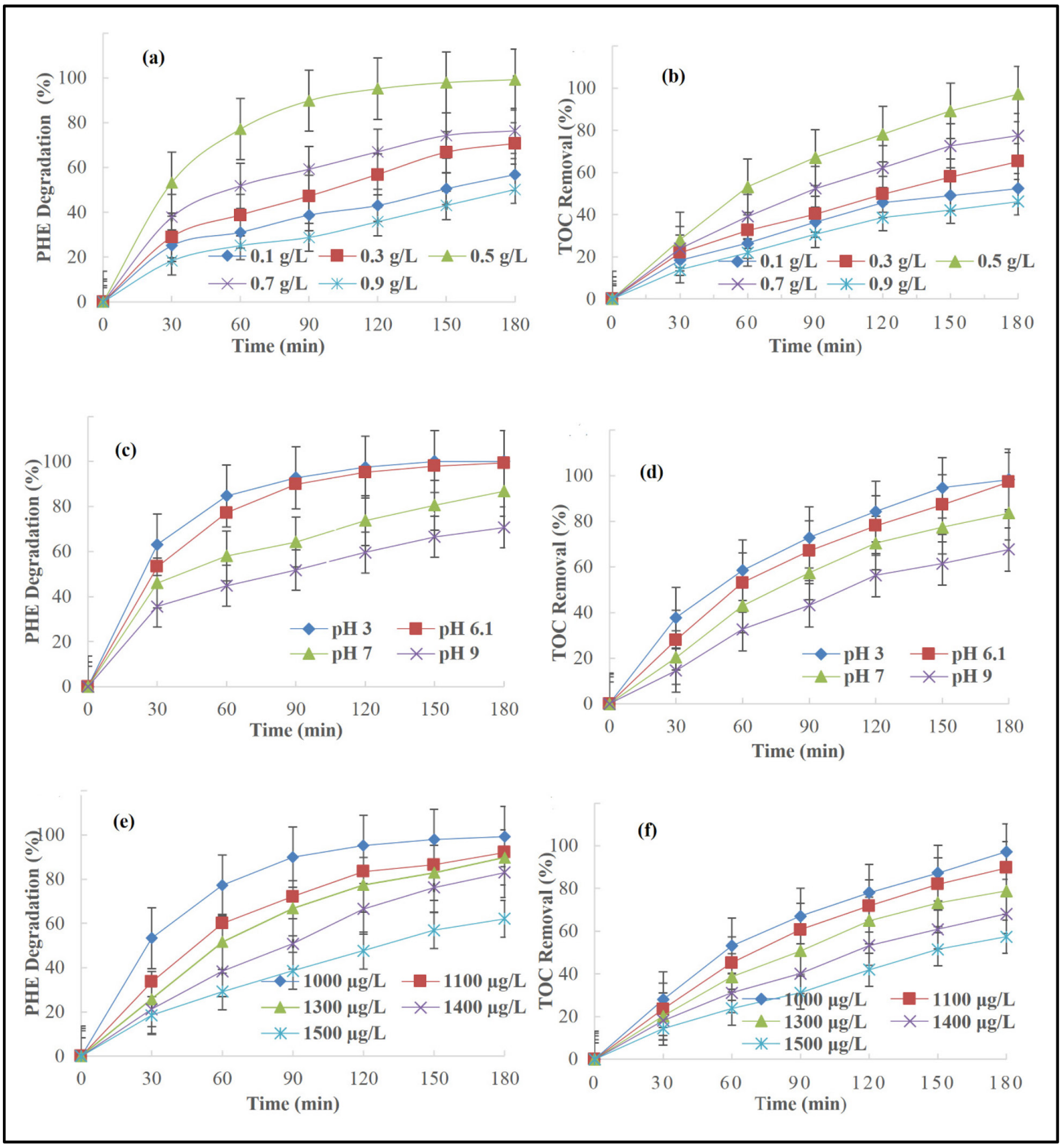

Fig. 2. Effect of TiO_2 dosage, feed solution pH and initial PHE concentrations on PHE degradation (a), (c) and (e) and TOC removal (b), (d) and (f); [PHE] = 1000 µg/L, $[TiO_2]$ = 0.5 g/L, Time = 3 h.

photocatalytic UF membrane process is very complex because of its multiple roles such as electrostatic interactions between catalyst surface, PHE, charged radicals and membrane surface [26].

The point of zero charge (P_{zc}) of TiO_2 P25 is 6.8. The catalyst surface was positively charged in acidic solutions ($P_{zc} < 6.8$) and negatively charged in alkaline solution ($P_{zc} > 6.8$).The greater PHE degradation and mineralization at acidic pH was due to the strong affinity of PHE molecules on the TiO_2 surface because of electrostatic interactions. This facilitates the attack of hydroxyl radicals formed on the photon-activated catalyst surface for the degradation of PHE molecules. On the contrary, as the pH increases and is > 6.8, the TiO_2 surface gradually becomes negatively charged and develops more repulsive forces between TiO_2 surface and PHE molecules and thereby retarding the adsorption of PHE molecules on the TiO_2 surface. Hence at alkaline pH, the hydroxyl radicals have to diffuse away from the particles to degrade the compound in the solution. In this study, lower percentage removal of 71% was obtained at pH = 9. These results were in agreement with the results obtained by others during photocatalytic processes [47,49,50].

During membrane separation, adsorption plays major role for PHE removal. In addition, the hydrophobicity of PHE molecules (Log $K_{ow} > 4$) would also have caused for the retention of PHE molecules by UF membrane and increased the removal efficiency.

However in PMR, the zeta potential and agglomerated sizes of TiO_2 would have probably enhanced the rejection of PHE that were adsorbed onto TiO_2 particles by UF mem-

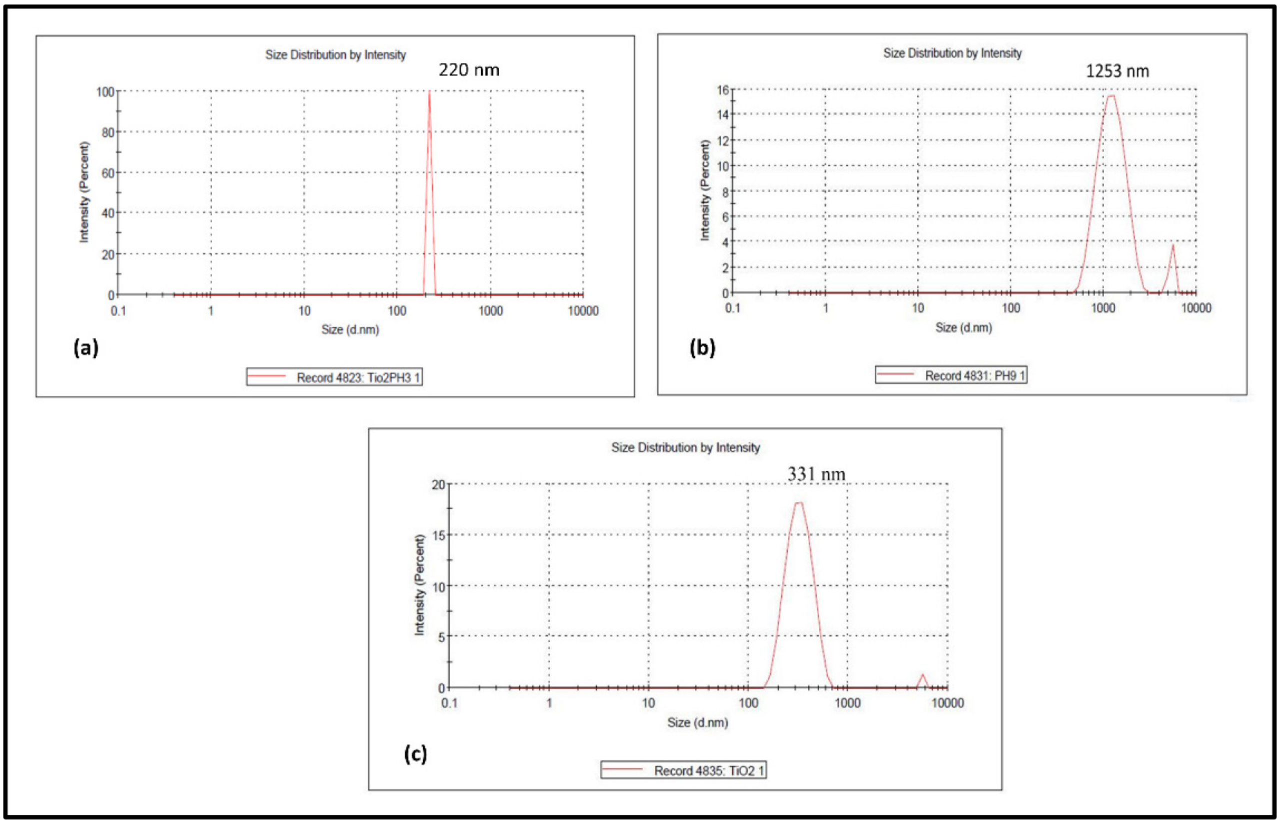

Fig. 3. DLS measurements of agglomerated sizes of TiO_2 for various feed pH (a) pH = 3; (b) pH = 9; (c) pH = 6.1.

branes thus contributing to increase in removal efficiency. Moreover, the charge characteristics of UF membrane including surface zeta potential as a function of feed water pH remains still unclear [24,51].

From the preceding discussions we can conclude that controlling pH (in the acidic range) in PMRs could improve the degradation rate during PCO process.

3.4.3. *Effect of PHE initial concentrations on photocatalytic degradation and its kinetics*

The effect of initial PHE concentrations on percent removal was studied in a batch reactor by varying the initial concentrations of PHE from 1000 µg/L to 1500 µg/L with 0.5 g/L TiO_2 dosage for 3 h and the results are shown in Figs. 2e and f. The samples were collected at every 30 min intervals and PHE concentrations were analysed by GC-MS. It can be seen from Figs. 2e and f that as the initial PHE concentration increased (from 1000 µg/L to 1500 µg/L), both percent degradation (from 99.3 to 68.9%) and mineralization (TOC) (from 97.2 to 57.4%) decreased. The possible explanation for this behaviour is that when the initial PHE concentration was increased, more and more PHE molecules were adsorbed onto TiO_2 surface. This increases the requirement of reactive species ($^{\bullet}OH$ and $^{\bullet}O_2^-$) to degrade PHE molecules. Since the light intensity, irradiation time and catalyst dosage are constant, the amount of hydroxyl radicals formed on the TiO_2 surface also remains constant. Hence, the available reactive species were inadequate for PHE degradation at higher initial concentrations which in turn reduces the PHE degradation rate at higher initial concentrations [52]. Similar observations were made by others for dye removal [25,53].

Furthermore, the steeper slope in the figure indicates that the rate of PHE removal was initially higher and slowed down at higher concentrations. The initial steeper trend may be due to the availability of sufficient catalyst surface for PHE degradation at early stages. However, the intermediate compounds which were formed during the breakdown of compound molecules might have competed with the PHE molecules for active sites resulting in lowered rate of degradation at later stages. Similar behaviours were observed by others on dyes; Reactive Red 2 [44], Acid Red and Acid Green [54] and Reactive Black 5 [25]. In this study, the maximum percent removal of PHE and TOC removals of 99% and 97% were obtained when PHE concentration was 1000 µg/L. Hence, the optimum concentration was taken as 1000 µg/L.

The obtained experimental PHE removal data in this study could be fitted to pseudo-first-order kinetics with respect to the concentration of PHE [Eqs. (2) and (3)]

$$\frac{d[\mathrm{PHE}]_t}{dt} = k[PHE]_0 \tag{2}$$

$$\ln\frac{[\mathrm{PHE}]_0}{[\mathrm{PHE}]_t} = -kt \tag{3}$$

where $[PHE]_t$(µg/L) - concentration of PHE at time t; $[PHE]_0$(µg/L) - initial concentration of PHE; *t* (min) - reaction time and *k* (min^{-1}) - pseudo first order rate constant. First order rate constants were determined by regression analysis. Table 1S (Supplementary content) shows the pseudo-first-order rate constant (*k* and R^2 values) for different PHE concentrations. These results revealed that the initial PHE concentrations had significant influence on the degradation rate. The plot for $\ln[PHE]_0/[PHE]_t$ and $\ln [TOC]_0/[TOC]_t$ vs. *t* are shown in Figs. 4a and b. The calculated R^2 values (correlation coefficient) (shown in Table 1S - Supplementary content) confirm the pseudo first order kinetics of PHE removal. Furthermore, it was also observed that as the initial concentrations increased from 1000 µg/L to 1500 µg/L, the rate constant decreased from 0.028 to 0.00539 min^{-1}. This is due to the fact that as the PHE concentration increases, the path length of the photons entering the solution decreases. On the contrary, as the PHE concentration decreases, the path length for the photons increases [55]. Since the illumination time and amount of photocatalyst are constant, the reactive species (hydroxyl radicals and superoxide anions) attacking the PHE molecules decrease with increase in PHE concentration. Hence at higher concentration, the degradation and mineralization decreases due to the retardation of penetrating light [56]. Similar observations were made by others [29,57,58]. Damodar and You [29] investigated the degradation of RB5 in a slurry PMR and reported that an increase in RB5 concentration from 25 to 125 mg/L ($[TiO_2]$ = 0.5 g/L; 15 W, UC-C lamp; irradiation time = 5 h), decreased the degradation rate from 0.070 to 0.0211 min^{-1}. Laohapropanaon et al. [57] examined the degradation of RB5 in a slurry PMR and observed a rapid decrease in kinetic constant from 0.1981 to 0.0090 min^{-1} for an increase in RB5 concentration from 25 to 150 mg/L ([ZnO] = 1.25 g/L; Two low pressure UV-C lamps; irradiation time = 4 h). Sobana and Swaminathan [58] noticed a decrease in kinetic constant values during degradation of AR18 from 0.059 to 0.016 min^{-1} while increasing theA18 concentrations from 2 to 10 × 10^{-4} mol/L. The comparison of pseudo first order kinetic data for PHE degradation and TOC removal rates during UV-TiO_2 and UV-TiO_2 + Membrane processes are shown in Table 1S.

3.5. Comparison of PHE and TOC removal during individual and integrated processes

The graphical representation of comparative results (for optimized values) of PHE degradation, TOC removal and kinetic constants obtained during individual (membrane separation, UV-TiO_2) and integrated processes (UV-TiO_2 + membrane separation) are shown in Figs. 5a and b. During membrane separation, at initial stages, a rapid decrease in PHE concentration was observed. This was due to the fast adsorption of compound molecules on the membrane surface. Finally PHE removal was 53% after 3 h during membrane separation. During UV-TiO_2 process, maximum PHE degradation of 84% and TOC removal of 60% were obtained for the optimized parameters. The reduction in concentration of PHE during UV-TiO_2 process may be due to the destruction of compound molecules by hydroxyl radicals. Furthermore, 99% PHE and 97% TOC removals obtained during integrated experiments (UV-TiO_2 + Membrane separation) were found to be greater than other individual experiments. Less fouling observed on the membrane surface indicates that higher PHE removal was mainly due to the adsorption on the surface of TiO_2 not on the membrane surface. If the available adsorptive area of TiO_2 and membrane surface are considered, the adsorptive area during membrane photocatalytic processes (with an active surface area 50 m^2/g for P25) are 10000 times higher [26]. The comparative results of UV-TiO_2, Membrane and UV-TiO_2 + Membrane processes with various catalyst dosages and pH are depicted in Fig. 2S (Supplementary content). According to the results obtained, the higher *k* values with R^2 values greater than 0.9 at lower initial concentrations (1000 µg/L) indicates that lower initial concentrations favoured for greater removal of the target compound. During this study it was also noticed that the degradation rate was almost doubled during integrated process (UV-TiO_2 + membrane separation).

3.6. RSM modelling and optimization of photocatalytic degradation

In this work, the three parameters/factors such as pollutant concentration, TiO_2 dosage and pH were chosen as

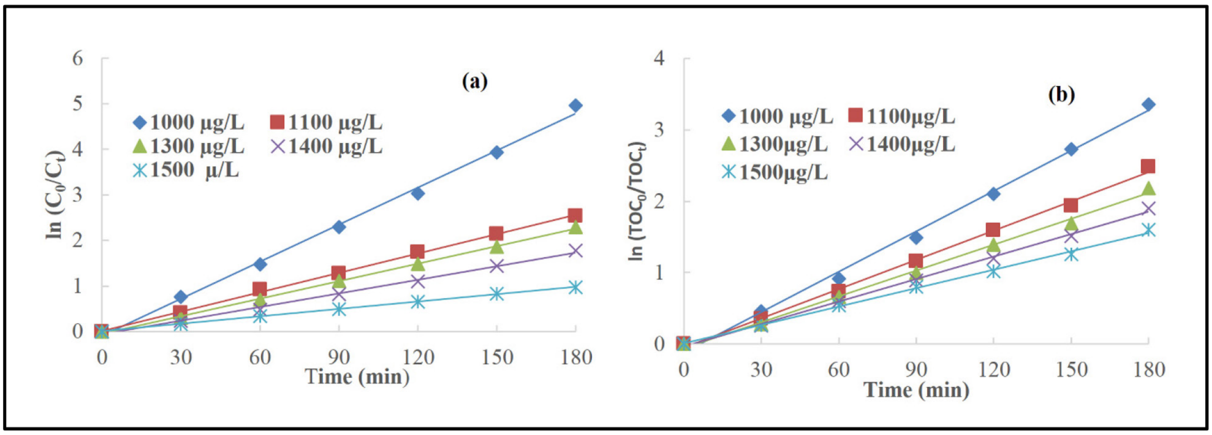

Fig. 4. The pseudo first order kinetic plot of (a) $\ln([PHE]_0/[PHE]_t)$ and (b) $([TOC]_0/[TOC]_t)$ vs. time for PHE.

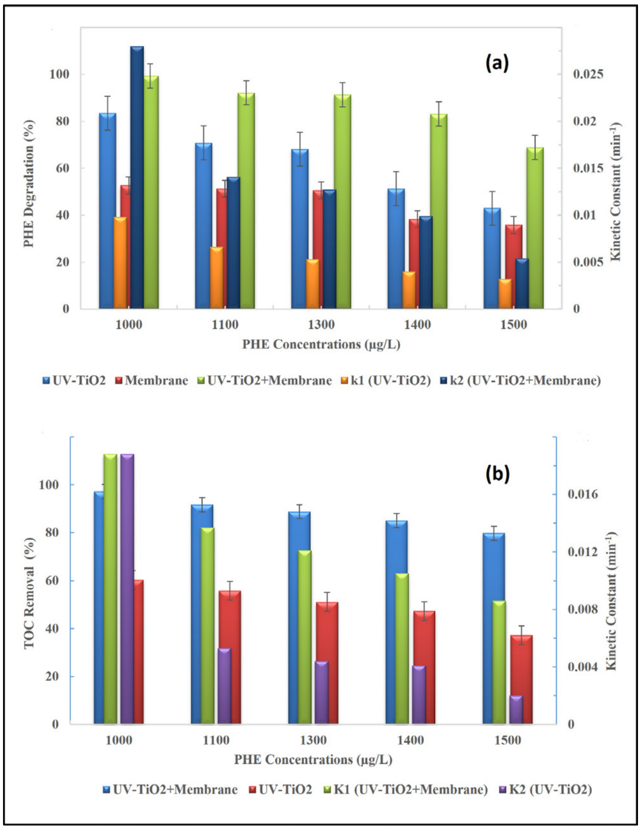

Fig. 5. Comparative results of (a) PHE degradation and (b) TOC removal including pseudo first order reaction constants during individual and integrated processes.

independent variables while PHE degradation (%) (Y_1) and TOC removal (%) (Y_2) were chosen as responses. Based on the CCD matrix and the experimental data (for the UV-TiO_2 + membrane processes), two second order polynomial expressions were obtained and are shown in Eqs. (4) and (5).

$$\text{PHE degradation (\%)} \ (Y_1) = +94.42 - 14.72{*}x_1 - 2.31{*}x_2 - 14.21{*}x_3 - 20.60 * x_1^2 - 35.26 {*}x_2^2 \tag{4}$$

$$\text{TOC removal (\%)} \ (Y_2) = 83.64 - 16.33 * x_1 + 0.63 {*}x_2 - 14.88 * x_3 - 13.44 {*}x_1^2 - 35.97{*}x_3^2 \tag{5}$$

The parameters used in the CCD and the experimental data in the CCD for the study of photodegradation of PHE are shown in Tables 1 and 2.

The significance and adequacy of the model was tested by ANOVA (Analysis of variance). The ANOVA results of quadratic model for PHE degradation and TOC removal efficiencies are shown in Tables 2S and 3S (Supplementary content). F-values greater than unity and probability values lesser than 0.0001 revealed that the models obtained were highly significant. The model large F-value (27.75 and 27.97 for PHE degradation and TOC removal efficiencies) and "Prob > F" less than 0.0500 indicate that the model terms are significant and only 0.01% chance that this could occur due to noise. Moreover, the adequate precision value (14.293 and 14.446) for PHE degradation and TOC removal percentages > 4 also confirm the adequacy of the model. It can also be seen a good correlation between the experimental data and the predicted values and hence the data fitted well with the range studied. This could be confirmed with the normal probability plot of residuals (Figs. 6a and c) and the plot of residuals vs predicted response (Figs. 6b and d). The residuals fallen on a straight line suggested that the errors are distributed normally.

Table 1
Parameters used in central composite design

Parameter	Symbol	Low (–1)	Center (0)	High (+1)
x_1	PHE conc (Micrograms per Litre)	1000	1250	1500
x_2	Catalyst dosage (g/L)	0.1	0.5	0.9
x_3	pH	3	9	6

The three dimensional response surface plots shown in Figs. 7a–d are the graphical representation of the regression Eqs. (4) and (5). An increase in PHE degradation was observed with increase in TiO_2 dosage. However with the increased number of active sites, a decrease in efficiency was observed at high values of TiO_2 dosage. This may be due to the light screening and scattering effects as well as the agglomeration of the catalyst particles which caused for the decrease in efficiency [54,59,60]. The degradation efficiency did not increase after 0.5 g/L (optimum value) of TiO_2. On the contrary, increase in PHE concentration, showed negative effect on degradation and TOC removal efficiency. This may be due to the inadequate availability of reactive species (hydroxyl radicals) as their amount needed is more at higher concentrations. Furthermore, at acidic pH, the higher PHE and TOC removalS may be due to the surface charge of TiO_2. Similar observations were made by various authors for different compounds such as dyes (acid blue 92 and basic blue 3) [61] and triclosan [62].

The effects of three factors studied for the removal of PHE and TOC are shown in Figs. 7a–d. The optimization software with desirability approach was utilized to find the specific points that maximize PHE and TOC removal percentages. The highest PHE removal and TOC removals were obtained at the operating conditions of 1000 µg/L of PHE, 0.5 g/L of TiO_2 and pH of 3.

4. Conclusion

A submerged slurry PMR was evaluated for PHE removal and the maximum PHE and TOC removals obtained were 99.3% and 97.2% for optimized conditions ([PHE] = 1000 µg/L, [TiO_2] = 0.5 g/L, pH = 3) during batch studies. The rate of PHE and TOC removals obtained during integrated process (UV-TiO_2 + membrane process) in PMR was almost 15% and 37% greater than the conventional UV-TiO_2 process and the PMR was efficient to mineralize PHE. Initial PHE concentrations had significant influence on PHE degradation and the maximum degradation was obtained at lower initial concentration

Table 2
Experimental data in the central composite design for the study of the photodegradation of PHE

Run	Block	Factor 1 A: PHE concentration (μg/L)	Factor 2 B: Catalystdosage (g/L)	Factor 3 pH	Response 1 PHE degradation %	Response 2 TOC removal %
1	Block 1	1000.00	0.50	6.10	99.3	97.2
2	Block 1	1100.00	0.50	6.10	92.1	89.7
3	Block 1	1300.00	0.50	6.10	89.62	78.8
4	Block 1	1400.00	0.50	6.10	83.1	68.1
5	Block 1	1500.00	0.10	6.10	62.1	57.4
6	Block 1	1000.00	0.30	6.10	56.9	52.4
7	Block 1	1000.00	0.50	6.10	70.7	65.4
8	Block 1	1000.00	0.70	6.10	76.35	68.5
9	Block 1	1000.00	0.90	6.10	50.2	47.0
10	Block 1	1000.00	0.50	3.00	100	98.3
11	Block 1	1000.00	0.50	7.00	86.6	83.6
12	Block 1	1000.00	0.50	9.00	70.5	67.6
13	Block 2	1000.00	0.50	6.10	99.3	97.2
14	Block 2	1300.00	0.50	6.10	89.6	78.8
15	Block 2	1500.00	0.50	6.10	52.4	49.8
16	Block 2	1000.00	0.10	6.10	56.8	46.2
17	Block 2	1000.00	0.90	6.10	50.3	47.2
18	Block 2	1000.00	0.50	3.00	99.1	98.4
19	Block 2	1000.00	0.50	7.00	83.7	83.9
20	Block 2	1000.00	0.50	9.00	70.5	67.8

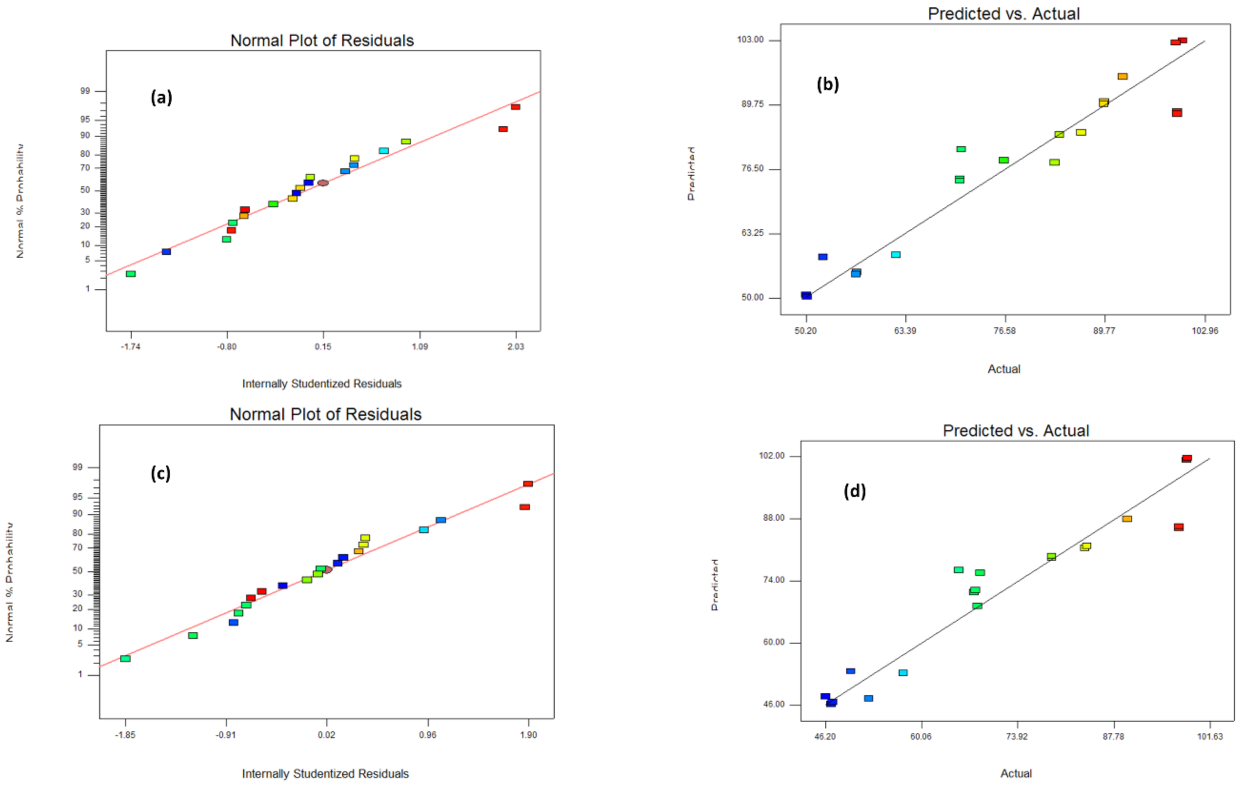

Fig. 6. Normal probability plot of residuals and predicted vs. actual values for photocatalytic degradation of PHE [(a) and (b) and TOC removal [(c and (d)]].

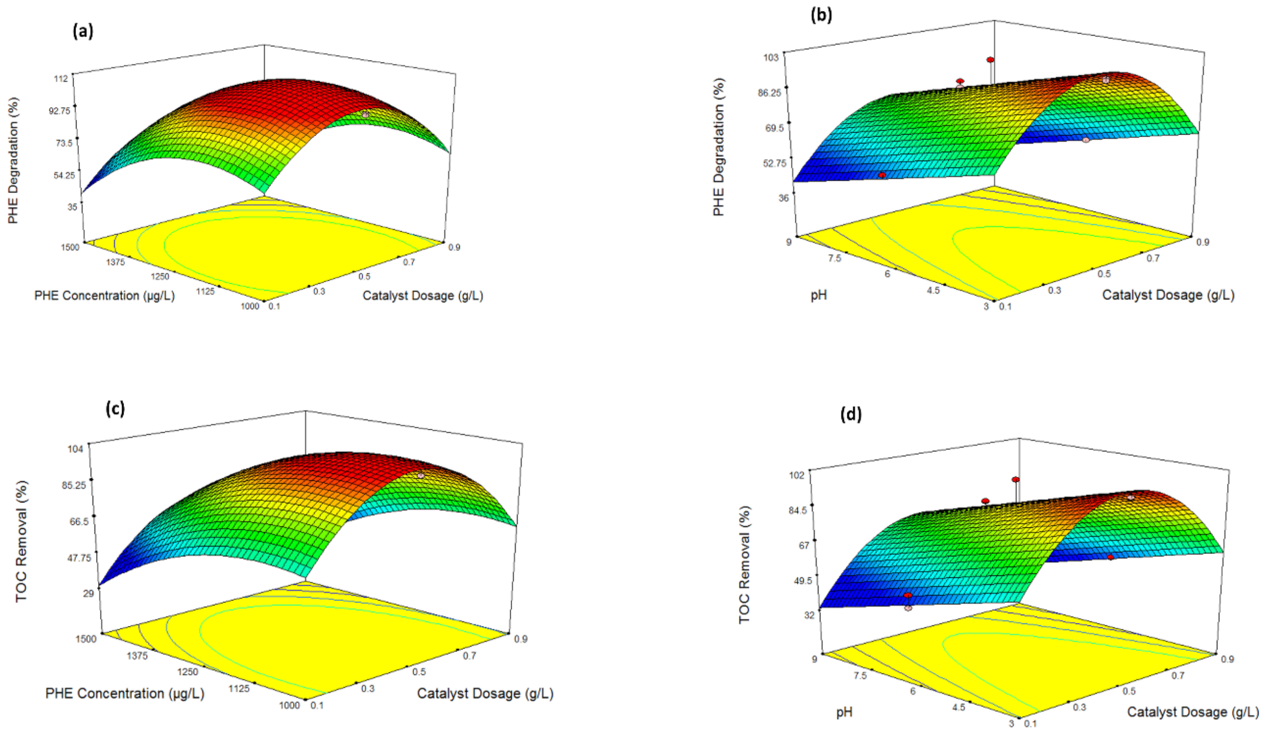

Fig. 7. Response surface methodology 3D surface plots for PHE removal (a), (b) and TOC removal (c), (d).

and pH. The experimental data was fitted to pseudo first order kinetics. RSM modelling using Design expert software was used to analyse the obtained experimental data. ANOVA with high coefficients of correlation ($R^2 = 0.9143$; Adjusted $R^2 = 0.8814$; predicted $R^2 = 0.8384$ for PHE degradation and $R^2 = 0.9150$; Adjusted $R^2 = 0.8822$; predicted $R^2 = 0.8419$ for TOC removal) confirmed the good agreement between the experimental and predicted values. Furthermore, the 3D surface plots of RSM revealed that all the operating parameters studied had significant impact on PHE removal.

Acknowledgements

The authors would like to acknowledge University Grants Commission (UGC), New Delhi, India for rendering financial support while carrying out this research work.

Conflict of Interest

The authors declare that they have no conflict of interest.

References

[1] C.N. Rani, S. Karthikeyan, Endocrine disrupting compounds in water and wastewater and their treatment options - a review, Int. J. Environ. Technol. Manage., 19(5/6) (2016) 392–431.

[2] IARC, International Agency for Research on Cancer. Monographs on the evaluation of carcinogenic risk of chemicals to humans. Overall evaluation of carcinogenity: An updating of IAPC monographs, Int. Agency for res. on cancer-France, 1–42 (1987) Suppl. 7.

[3] Y. Jian, L. Wan, P.F. Peter and H.T. Yu, Photomutagenicity of 16 polycyclic aromatic hydrocarbons from the US EPA priority pollutant list, Mutat. Res., 557 (2004) 99–108.

[4] H.I. Abdel-Shafy and M.S.M. Mansour, A review on polycyclic aromatic hydrocarbons: Source, environmental impact, effect on human health and remediation, Egt. J. Petroleum, 25 (1) (2016) 107–123.

[5] K. Kozak, M. Ruman, K.Kosek, G. Karasi, L. Stanchnik and Z. Polkowska, Impact of volcanic eruptions on the occurrence of PAHs compounds in the aquatic ecosystem of the southern part of West Spitsbergen (Hornsund Fjord, Svabard), Water, 9 (42) (2017) 1–21.

[6] N. Vela, M. Martinez-Menchon, G. Navarro, G. Parez-Lucas and S. Navarro, Removal of polycyclic aromatic hydrocarbons (PAHs) from ground water by heterogeneous photocatalysis under natural sunlight, J. Photochem. Photobiol. A: Chem., 232 (2012) 32–40.

[7] E. Lipiatou, J. Tolosa, R. Simo, I. BouloubDachs, S. Marti, M.A. Sicre, J.M. Bayona, J.O. Grimalt, A. Saliot and J.J. Albaiges, Mass budget and dynamics of polycyclic aromatic hydrocarbons in the Mediterranean Sea, Top. Stud. Oceanogr., 44 (1997) (881–905).

[8] U. Zoller, Groundwater contamination by detergents and polycyclic aromatic hydrocarbons - a global problem of organic contaminants: is the solution locally specific, Water Sci. Technol., 27 (1993) 187–194.

[9] K. Kveseth, B. Sortland and T. Bokn, Aromatic hydrocarbons in sewage mussels and tap water, Chemosphere, 11 (1982) 623–639.

[10] V.S. Gowri, R. Ramesh, P. Nammalwar, N. Satheesh, J. Rajkumar, Kakolee Banerjee andSeshaBamini, GIS approach in assessing the status of neritic water quality and petroleum hydrocarbons in Bay of Bengal (From Chennai to Nagapattinum, Tamil Nadu), India, Int. J. Geomatics and Geosci., 3 (1) (2012) 248–257.

[11] K. Brindha and L. Elango, PAHs contamination in groundwater from a part of metropolitan city, India: a study based on sampling over a 10-year period, Environ Earth Sci., 7 (12) (2014) (5113–5120).

[12] S. Malakar, P. DasSaha, Estimation of VOC emission in petroleum refinery ETP and comparative analysis with measured VOC emission rate, Int. J. Eng. Sci., 4(10) (2015) 20–29.

[13] H.F. Lin, K.T. Valsaraj, A titania thin film annular photocatalytic reactor for the degradation of polycyclic aromatic hydrocarbons in dilute water streams, J. Hazard. Mater., 99 (2003) 203–219.

[14] S. Wen, J.C. Zhao, G.Y. Sheng, J.M. Fu, P.A. Peng, Photocatalytic reactions of phenanthrene at TiO_2/water interfaces, Chemosphere, 46 (2002) 871–877.

[15] B. Liu, B. Chen, B.Y. Zhang, L. Jing, Photocatalytic degradation of polycyclic aromatic hydrocarbons in offshore produced water: Effects of water matrix, J. Environ. Eng., 142(11) (2016) 04016054 (1–7).

[16] S. Sanches, C. Leitao, A. Penetra, V.V. Cardoso, E. Ferreira, M.T. Benoliel, B. Crespo, V.J. Pereira, Direct photolysis of polycyclic aromatic hydrocarbons in drinking water sources, J. Hazard. Mater., 192(3) (2011) 1458–1465.

[17] S.A. Snyder, S. Adham, A.M. Redding, F.S. Cannon, J. DeCarolis, J. Oppenheimer, E.C. Wert, Y. Yoon, Role of membranes and activated carbon in the removal of endocrine disruptors and pharmaceuticals, Desalination, 202 (2007) 156–181.

[18] C.P. Huang, C. Dong, Z. Tang, Advanced chemical oxidation: Its present role and potential future in hazardous waste treatment, Waste Manage., 13 (1993) 361–377.

[19] M.Y. Ghaly, T.S. Jamila, I.E. El-Seesy, E.R. Souaya, R.A. Nasr, Treatment of highly polluted paper mill wastewater by solar photocatalytic oxidation with synthesized nanoTiO_2, Chem. Eng. J., 168(1) (2011) 446–454.

[20] L.M. Ahmed, I. Ivanova, F.H. Hussein, D.W. Bahnemann, Role of platinum deposited on TiO_2 in photocatalytic methanol oxidation and dehydration reactions, Int. J. Photoenergy, Article ID 503516 (2014) 1–9.

[21] M.A. Callahan, M.W. Slimak, N.W. Gabelc, I.P. May, C.F. Fowler, J.R. Freed, P. Jennings, R.L. Durfee, F.C Whitemore, B. Maestri, W.R. Mabey, B.R. Holt, C. Gloud, Water related environmental fate of 129 priority pollutants, Report no. EPA-440/4-79-029 (Washington, DC: US Environmental Protection Agency, 1979).

[22] S. Mozia, Photocatalytic membrane reactors (PMRs) in water and wastewater treatment, Sep. Purif. Technol., 73 (2010) 71–91.

[23] V. Augugliaro, M. Litter, L. Palmisano, J. Soria, The combination of heterogeneous photocatalysis with chemical and physical operations: A tool for improving the photoprocess performance, J. Photochem. Photobiol. C., 7 (2006) 127–144.

[24] V.C. Sarasidis, K.V. Plakas, S.I. Patsios, A.J. Karabelas, Investigation of diclofenac degradation in a continuous photocatalytic membrane reactor. Influence of operating parameters, Chem. Eng. J., 239 (2014) 299–311.

[25] R.A. Damodar, S.-J. You, S.H. Qu, Coupling of membrane separation with photocatalytic slurry reactor for advanced dye wastewater treatment, Sep. Purif. Technol., 76(1) (2010) 64–71.

[26] R.L. Fernandez, J.A. McDonald, S.J. Khan, P. Le-Clech, Removal of pharmaceuticals and endocrine disrupting chemicals by a submerged membrane photocatalysis reactor (MPR), Sep. Purif. Technol., 127 (2014) 131–139.

[27] A. Rahimpour, S.S. Madaeni, A.H. Taheri, Y. Mansourpanah, Coupling TiO_2 nanoparticles with UV irradiation for modification of polyether sulfone ultrafiltration membranes, J. Membr. Sci., 313 (2008) 158–169.

[28] D. Qu, Z. Qiang, S. Xiao, Q. Liu, Y. Lei, T. Zhou, Degradation of reactive black 5 in a submerged photocatalytic reactor with microwave electrodeless lamps as light source, Sep. Purif. Technol., 122 (2014) 54–59.

[29] R.A. Damodar, S.J. You, Performance of an integrated membrane photocatalytic reactor for the removal of Reactive Black 5, Sep. Purif. Technol., 71 (2010) 44–49.

[30] H. Jiang, G. Zhang, T. Huang, J. Chen, Q. Wang, Q. Meng, Photocatalytic membrane reactor for degradation of acid red B wastewater, Chem. Eng. J., 156 (2010) 571–577.

[31] C.N. Rani, S. Karthikeyan, Performance of an indigenous integrated slurry photocatalytic membrane reactor (PMR) on the removal of aqueous phenanthrene (PHE), Water Sci. Technol., 77(11) (2018) 2642–2656.

[32] S.S. Chin, T.M. Lim, K. Chiang, A.G. Fane, Factors affecting the performance of a low pressure submerged membrane photocatalytic reactor, Chem. Eng. J., 130 (2007a) 53–63.

[33] H. Zhu, D. Chen, D. Dong, Photolysis of phenanthrene on soil surfaces under UV-irradiation, Asian. J. Chem., 27(1) (2015) 101–105.

[34] P. Xu, J.E. Drewes, T.U. Kim, C. Bellona, G. Amy, Effect of membrane fouling on transport of organic contaminants in NF/RO membrane applications, J. Membr. Sci., 279 (2006) 165–175.

[35] S. Hajibabania, A. Verliefde, J.A. McDonald, S.J. Khan, P. Le-Clech, Fate of trace organic compounds during treatment by nanofiltration, J. Membr. Sci., 373 (2011) 130–139.

[36] K. Luks-Betlej, M. Dudziak, Membrane techniques in water treatment processes: Removal of polycyclic aromatic hydrocarbons and phthalates using nanofiltration, Ecohydrol. Hydrobiol., 5 (2005) 93–99.

[37] M. Smol, Wlodarczyk-Makula, Effectiveness in the removal of polycyclic aromatic hydrocarbons from industrial wastewater by ultrafiltration technique, Arch. Environ. Protection, 38(4) (2012) 49–58.

[38] C. Gong, H. Huang, Y. Qian, Z. Zhang, H. Wu, Integrated electrocoagulation and membrane filtration for PAH removal from realistic industrial wastewater: effectiveness and mechanisms, RSC Adv., 7 (2017) 52366–52374.

[39] O.R.S. da Rocha, R.F. Dantas, M.M.M.B. Duarte, M.M.L. Duarte, V.L. da Silva, Oil sludge treatment by photocatalysis applying black and white light, Chem. Eng. J., 157(1) (2010) 80–85.

[40] O.T. Woo, W.K. Chung, K.H. Wong, A.T. Chow, P.K. Wong, Photocatalytic oxidation of polycyclic aromatic hydrocarbons: Intermediates identification and toxicity testing, J. Hazard. Mater., 168 (2009) 1192–1199.

[41] M.J. Garcia-Martinez, L. Canoira, G. Blazquez, I. Da Riva, R. Alcantara, J.F. Llamas, Continuous photodegradation of naphthalene in water catalysed by TiO_2 supported on glass Raschig rings, Chem. Eng. J., 110 (2005) 123–128.

[42] H.K. Shon, S. Vigneswaran, H.H. Ngo, J.H. Kim, Chemical coupling of photocatalysis with flocculation and adsorption in the removal of organic matter, Water Res., 39 (2005) 2549–2558.

[43] D.P. Ho, S. Vigneswaran, H.H. Ngo, Photocatalysis-membrane hybrid system for organic removal from biologically treated sewage effluent, Sep. Purif. Technol., 68 (2009) 145–152.

[44] B. Neppolian, H.C. Choi, S. Sakthivel, B. Arabindoo, V. Murugesan, Solar/UV-induced photocatalytic degradation of three commercial textile dyes, J. Hazard. Mater., 89 (2–3) (2002) 303–317.

[45] K. Sopajaree, S.A. Qasim, S. Basak, K. Rajeshwar, An integrated flow reactor-membrane filtration system for heterogeneous photocatalysis. Part II: Experiments on the ultrafiltration unit and combined operation, J. Appl. Electrochem., 29(9) (1999) 1111–1118.

[46] S. Mozia, A.W. Morawski, Hybridization of photocatalysis and membrane distillation for purification of wastewater, Catalysis Today, 118 (1–2) (2006) 181–188.

[47] R. Wang, D. Ren, S. Xia, Y. Zhang, J. Zhao, Photocatalytic degradation of Bisphenol A (BPA) using immobilized $TiO_2$and UV illumination in a horizontal circulating bed photocatalytic reactor (HCBPR), J. Hazard. Mater., 169 (2009) 926–932.

[48] M.N. Chong, B. Jin, C.W.K. Chow, C. Saint, Recent developments in photocatalytic water treatment technology: A review, Water Res., 44(10) (2010) 2997–3027.

[49] K. Chiang, T.M. Lim, L. Tsen, C.C. Lee, Photocatalytic degradation and mineralization of bisphenol A by TiO_2 and platinized TiO_2, Appl. Catal., A, 261 (2004) 225–237.

[50] S.S. Chin, T.M. Lim, K. Chiang, A.G. Fane, Hybrid low-pressure submerged membrane photoreactor for the removal of bisphenol A, Desalination, 202 (2007b) 253–261.

[51] S.I. Patsios, V.C. Sarasidis, A.J, Karabelas, A hybrid photocatalysis-ultrafiltration continuous process for humic acids degradation, Sep. Sci. Technol., 104 (2013) 333–341.

[52] W. Bahmemann, M. Muneer, M.M. Haque, Titanium dioxide-mediated photocatalysed degradation of few selected organic pollutants in aqueous suspensions, Catal. Today, 124 (2007) 133–148.

[53] I.K. Konstantinou, T.A. Albanis, TiO_{2-} assisted photocatalytic degradation of azo dyes in aqueous solution: kinetic and mechanistic investigations: a review, Appl. Catal., B, 49 (2004) 1–14.

[54] M. Saquib, M. Muneer, Photocatalytic degradation of CI Acid Green 25 CI Acid Red 88 in aqueous suspensions of titanium dioxide, Color. Technol., 118 (2002) 307–315.

[55] R.J. Davis, J.L. Gainner, G.O. Neal, I. Wenwu, Photocatalytic decolourization of wastewater dyes, Water Environ. Res., 66 (1994) 50–53.

[56] L. Zhang, C.Y. Liu, X.M. Ren, Photochemistry of semiconductor particles. Part 4- Effects of surface condition on the photodegradation of 2, 4-dichlorophenol catalysed by TiO_2 suspensions, J. Photochem. Photobiol. A, 85 (1995) 239–245.

[57] S. Laohaprapanon, J. Matahum, L. Tayo, S-J. You, Photodegradation of Reactive Black 5 in a ZnO/UV slurry membrane reactor, J. Taiwan Inst. Chem. Eng., 49 (2015) 136–141.

[58] N. Sobana, M, Swaminathan, Three effects of operational parameters on the photocatalytic degradation of acid red 18 by ZnO, Sep. Purif. Technol., 56 (2007) 101–107.

[59] M. Antonopoulou, V. Papadopoulos, I. Konstantinou, Photocatalytic oxidation of treated municipal wastewaters for the removal of phenolic compounds: optimization and modelling using response surface methodology (RSM) and artificial neural networks (ANNs), J. Chem. Technol. Biotechnol., 87(10) (2012) 1385–1395.

[60] C.N. Rani, S. Karthikeyan, Photocatalytic degradation of aqueous phenanthrene in a slurry photocatalytic reactor: optimization and modelling, Curr. Sci., 115(9) (2018) 1732–1740.

[61] M. Fathinia, A.R. Khataee, M. Zarei, S. Aber, Comparative photocatalytic degradation of two dyes on immobilized TiO_2 nanoparticles: Effect of dye molecular structure and response surface approach, J. Mol. Catal., A 333(1–2) (2010) 73–84.

[62] N. Stamatis, M. Antonoupoulo, D. Hela, I. Konstantinou, Photocatalytic degradation kinetics and mechanisms of antibacterial triclosan in aqueous TiO_2 suspensions under simulated solar irradiation, J. Chem. Technol. Biotechnol., 89(8) (2014) 1145–1154.

Supplementary Data

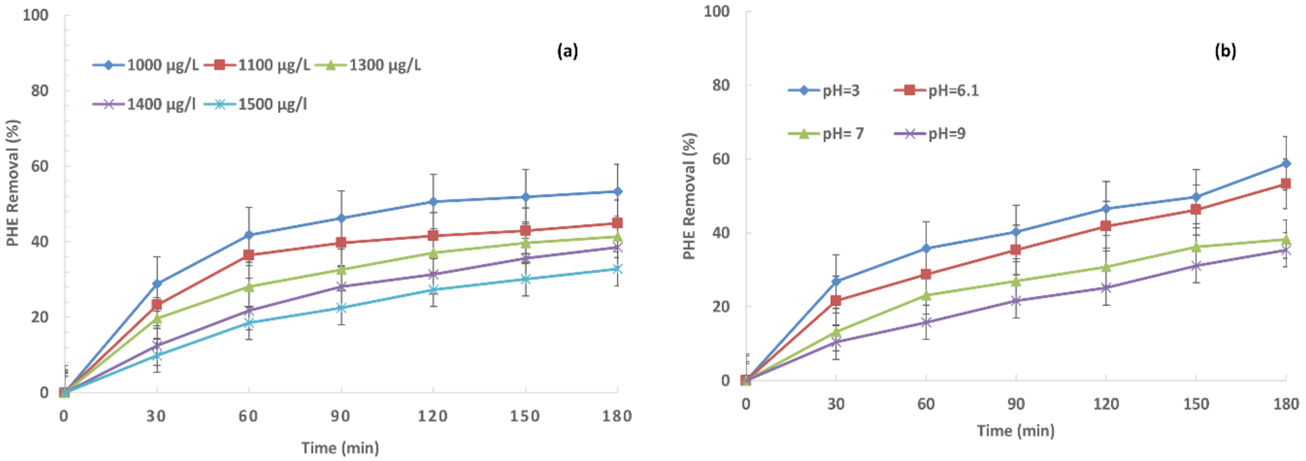

Fig. 1S. Effect of (a) Initial PHE concentrations and (b) pH on PHE removal during membrane separation; [PHE] = 1000 µg/L, Time = 3 h.

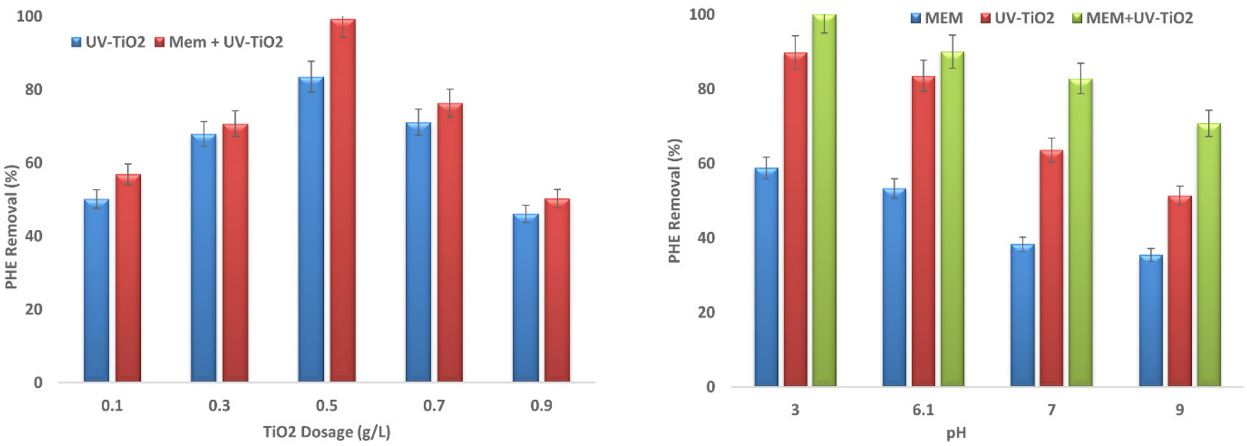

Fig. 2S. Comparison of PHE removals for the effect of (a) TiO_2 dosage and (b) pH during individual and integrated processes.

Table S1
Comparison of pseudo first order kinetic data the PHE degradation and TOC removal rates during UV-TiO_2 and UV-TiO_2 + Membrane processes

PHE Concentration (µg/L)	PHE Degradation				TOC Removal			
	(UV-TiO_2)		(UV-TiO_2) + Membrane		(UV-TiO_2)		(UV-TiO_2) + Membrane	
	K (min^{-1})	R^2	*K* (min^{-1})	R^2	*K* $(min)^{-1}$	R^2	*K* (min^{-1})	R^2
1000	0.0098	0.994	0.028	0.9965	0.0052	0.9847	0.0188	0.9954
1100	0.0066	0.9972	0.0141	0.9989	0.0053	0.9913	0.0137	0.997
1300	0.0053	0.9948	0.0127	0.9988	0.0044	0.9971	0.0121	0.9961
1400	0.004	0.9919	0.00989	0.9957	0.0041	0.9928	0.0105	0.9979
1500	0.0032	0.9904	0.00539	0.9994	0.002	0.9917	0.0086	0.9974

Table S2
ANOVA results of quadratic model for degradation of PHE (%) (Y_1)

Source	Sum of Squares	df	Mean Square	F Value	p-value prob> F	
Block	40.65	1	40.65			
Model	5382.30	5	1076.46	27.75	<0.0001	Significant
A-PHE Concentration	1574.26	1	1574.26	40.58	<0.0001	
B-Catalyst Dosage	23.92	1	23.92	0.62	0.4464	
C-pH	839.67	1	839.67	21.65	0.0005	
A^2	680.74	1	680.74	17.55	0.0011	
B^2	3350.54	1	3350.54	86.38	<0.0001	
Residual	504.27	13	38.79			
Lack of Fit	23.44	6	3.91	0.19	0.9581	Not significant
Pure Error	60.81	3	20.27			
Cor Total	5927.21	19				

Std. Dev. 6.23; Mean = 76.96; C.V % = 8.09; R^2 = 0.9143; Adj. R^2 = 0.8814; Pred.R^2 = 0.8384; Adeq Precision = 14.293

Table S3
ANOVA results of quadratic model for TOC Removal (%) (Y_2)

Source	Sum of Squares	df	Mean Square	F Value	p-value prob> F	
Block	13.10	1	13.40			
Model	5883.68	5	1176.74	27.97	<0.0001	Significant
A-PHE Concentration	1937.62	1	1937.62	46.06	<0.0001	
B-Catalyst Dosage	1.81	1	1.81	0.043	0.8391	
C-pH	921.35	1	921.35	21.90	0.0004	
A^2	289.85	1	289.85	6.89	0.0210	
B^2	409347	1	4093.47	97.30	<0.0001	
Residual	546.91	13	42.07			
Lack of Fit	186.82	8	23.35	0.42	0.8685	Not significant
Pure Error	278.61	5	55.72			
Cor Total	6443.99	19				

Std. Dev. 6.49; Mean = 72.17; C.V % = 8.99; R^2 = 0.9150; Adj. R^2 = 0.8822; Pred.R^2 = 0.8419; Adeq Precision = 14.446